Electronic Supplementary Material (ESI) for ChemComm.
This journal is © The Royal Society of Chemistry 2020

1. Experimental Section

Chemicals

Zinc nitrate hexahydrate, 1,4-benzenedicarboxylic acid, 1,4-diazabicyclo[2.2.2]octane, and *N*,*N*-dimethylformamide were purchased from FUJIFILM Wako Pure Chemical Corporation. 4-[4-(Dimethylamino)styryl]pyridine was purchased from Sigma-Aldrich Co. LLC.

Synthesis and degassing of 1

$Zn(NO_3)_2$•$6H_2O$ (250 mg, 0.84 mmol), 1,4-benzenedicarboxylic acid (H_2bdc; 140 mg, 0.84 mmol), and 1,4-diazabicyclo[2.2.2]octane (46.8 mg, 0.42 mmol) were dissolved in *N*,*N*-dimethylformamide (DMF; 10 mL) and vigorously stirred overnight. After the resulting white powder was removed by centrifugation, the supernatant solution was heated at 120 °C for 12 h in a Teflon-lined autoclave. The resulting crystals (**1**) were washed twice with DMF and then heated at 120 °C under vacuum.

Introduction of DMASP into 1

To introduce DMASP into **1**, guest-free **1** (30 mg) in a glass vial was placed into a Schlenk flask to which DMASP (80 mg) was added. The flask was then heated at 220 °C for 3 h. To see the effect of amount of DMASP in **1**, DMASP in a Schlenk flask was reduced to be 50 mg, while other conditions stayed same.

^{1}H-NMR of 1⊃DMASP

One drop of HCl_{aq} was added to **1⊃DMASP** to decompose the MOF crystals. The components of **1⊃DMASP** were dissolved in dimethyl sulfoxide-d_6 and analysed by ^{1}H-NMR.

Pulsed laser

The laser pulse wavelength, pulse width, repetition rate, and intensity were 355 nm, 300 ps, 1 kHz, and 0.4 mJ/cm^2, respectively. The spot size diameter was estimated to be approximately 80 μm. The supporting movie was edited by Adobe Premier Pro and played at 3.0 speed.

Continuous wave (CW) laser

The CW laser (coherent OBIS laser, 375 nm, 16 mW), ND filter (OD = 1.0), and objective lens (Plan Fluor 60×, N.A. 0.85, transmittance of approximately 80%

at 375 nm) were set to focus on **1**□**DMASP**. The spectra was recorded by iHR320 optical spectrometer (HORIBA, Ltd.).

Theoretical Calculations

Geometry optimization of the crystal structure of **1** was carried out using self-consistent charge density-functional tight-binding (SCC-DFTB)[S1] method with the third order expansion [S2] as implemented in the DFTB+ program package version 1.3.1.[S3] We employed 3ob parameters [S4] in all calculations with Hubbard derivatives (in atomic units) -0.1492 for C, -0.1857 for H, -0.1575 for O, -0.03 for Zn and -0.1535 for N. The atomic coordinates of C, H, O, N and Zn in **1** were optimized under periodic boundary condition including the Grimme's D3 type dispersion [S5] using reported crystal structure of **1** (CCDC 238860)[S6]. To evaluate the spatial position of DMASP in **1**, geometry optimization of model of **1**□**DMASP** with quantum mechanical (QM) and molecular mechanics (MM) calculations were performed using the ONIOM algorithm[S7, S8] as implemented in Gaussian 09.[S9] We performed two-layer ONIOM calculations, where the higher region includes the DMASP molecule and the lower region includes three sequential pores extracted from the optimized **1.** The dangling bonds of terephthalate and dabco were terminated with methyl groups and NH_3 molecules, respectively. QM calculations were carried out at the B3LYP/cc-pVDZ level of theory for the ground states and time-dependent B3LYP/aug-cc-pVDZ level of theory [S10] for the excited states. MM calculations were performed using the universal force field (UFF),[S11] where atomic charges were estimated at the initial geometry using the QEq algorithm.[S12] The ONIOM model was constructed from the optimized **1** by SCC-DFTB above mentioned. In order to include effects of the framework environment and keep the framework structure in the ONIOM model, the coordinates of Zn atoms were fixed at the positions in the structure of optimized **1**.

Instrumentation

SEM observation was conducted using a Phenom Pro desktop SEM system. XRD data were collected using a Rigaku SmartLab instrument. Laser scanning microscopy was performed using a Nikon A1 system with 405-nm laser. ^{1}H-NMR spectra were collected using a JEOL JNM-ECX400 spectrometer. Microscopic Raman spectroscopy was conducted using a Renishaw inVia spectrometer with 532 and 785-nm lasers. UV–vis absorption spectra were collected using JASCO V-750 spectrophotometer. Fluorescence spectra were collected using a Hitachi F-7000 spectrophotometer.

2. SEM images of 1

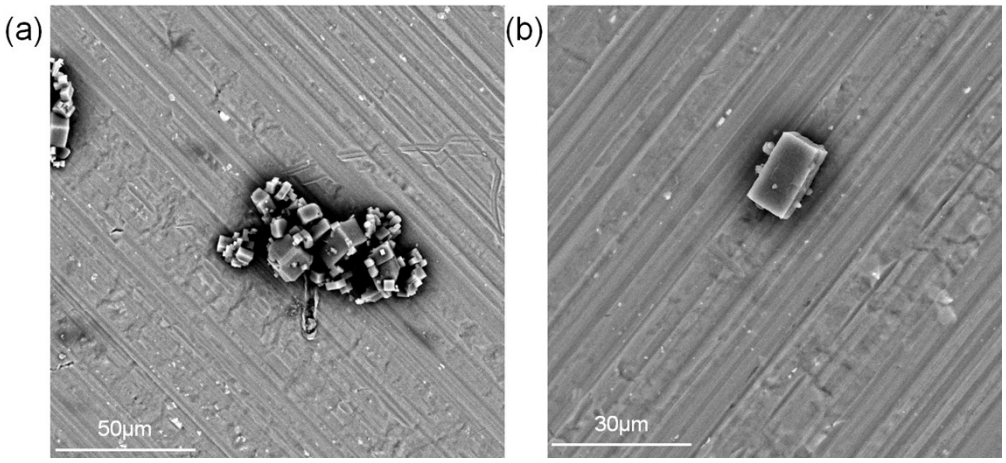

Figure S1. (a,b) SEM images of **1**.

3. XRD of 1□DMASP

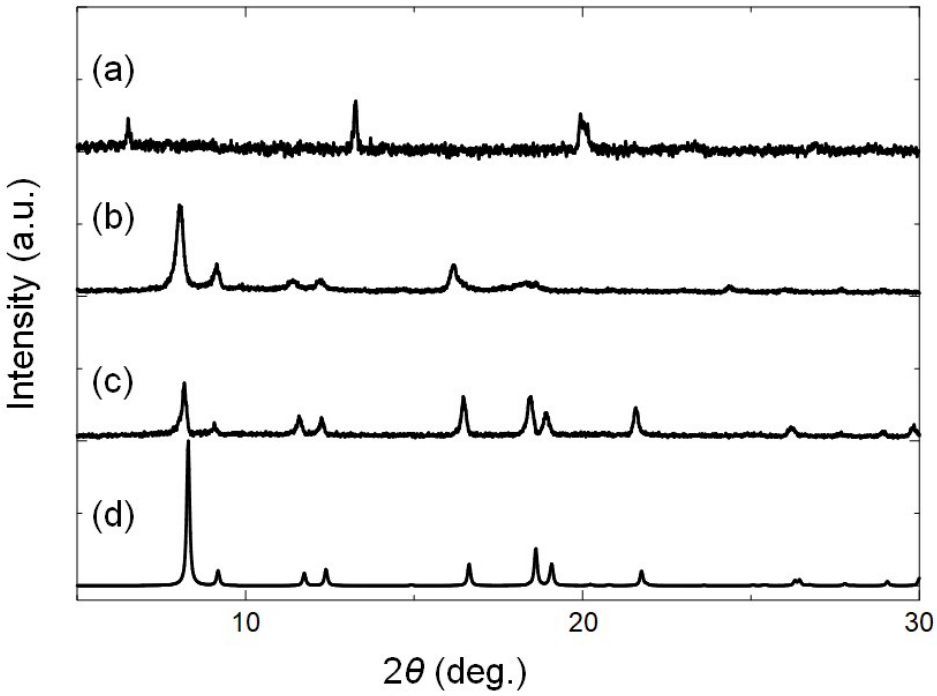

Figure S2. XRD patterns of (a) bare DMASP, (b) **1**□DMASP, (c) as-synthesized **1**, and (d) simulation of as-synthesized **1**.

4. ^{1}H-NMR of 1□DMASP

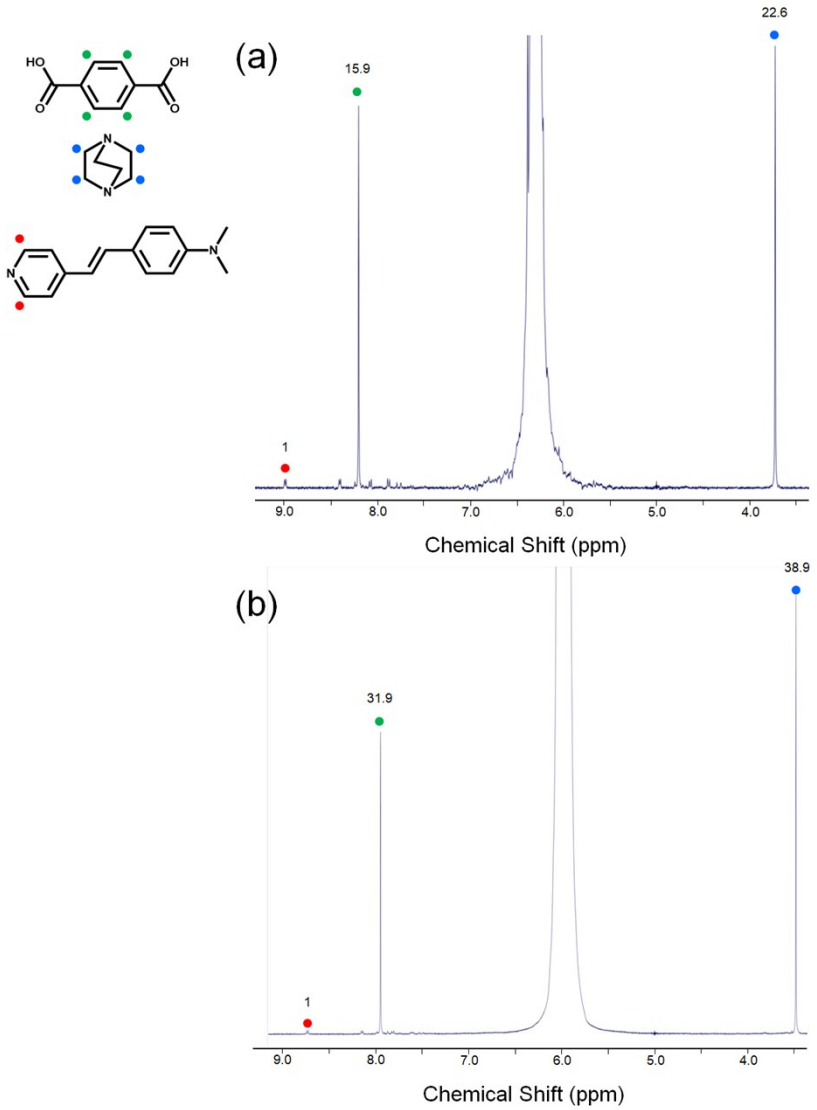

Figure S3. ^{1}H-NMR of digested (a) **1**□DMASP and (b) **1**□DMASP$_{half}$. Red, blue, and green dots are assigned to the protons of DMASP, dabco, and H_2bdc, respectively. Values adjacent to dots indicate the integral of each peak.

5. Fluorescence mechanism of DMASP

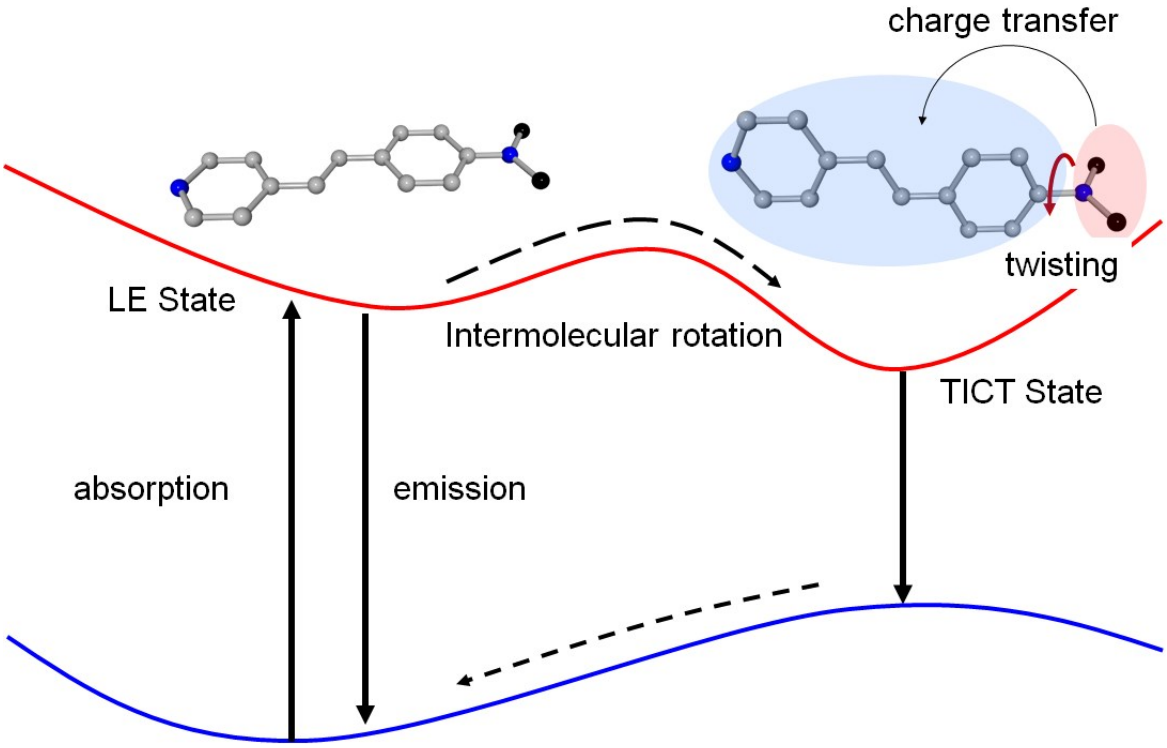

Figure S4. Schematic illustration of fluorescence mechanism of DMASP.

6. Fluorescent spectra of DMASP

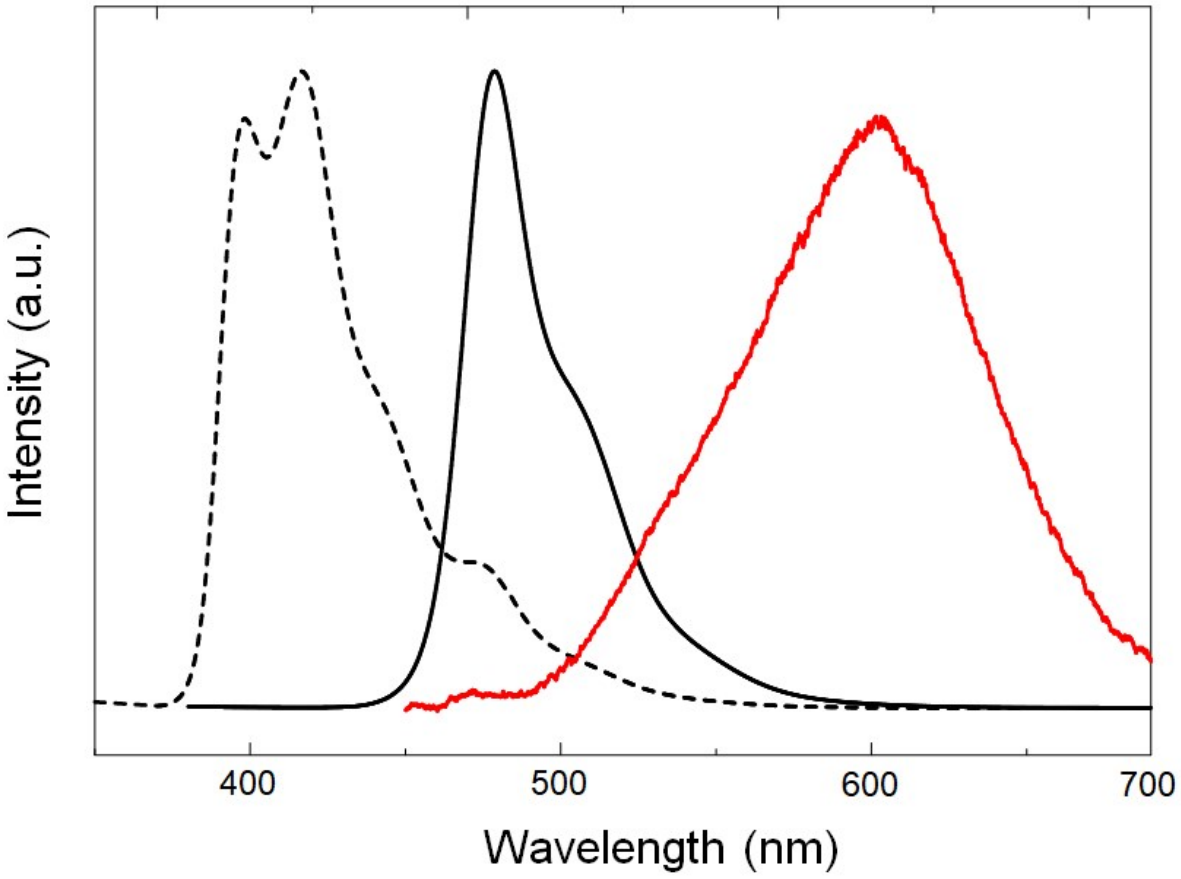

Figure S5. Fluorescent spectra of DMASP in hexane (black dot line), bare DMASP (black solid line), and **1**□DMASP (red line). Excitation wavelength is 355 nm.

The fluorescence wavelength of DMASP varied depending on the solvent polarity, as follows[S13]: 390–420 nm in hexane, 440 nm in dioxane, 490 nm in acetonitrile, 510 nm in methanol, and 550–660 nm in water (depending on pH). The emission from **1**□DMASP at around 600 nm indicated that DMASP was highly stabilized by the polarity of the pores.

7. Chronological change in fluorescent intensity

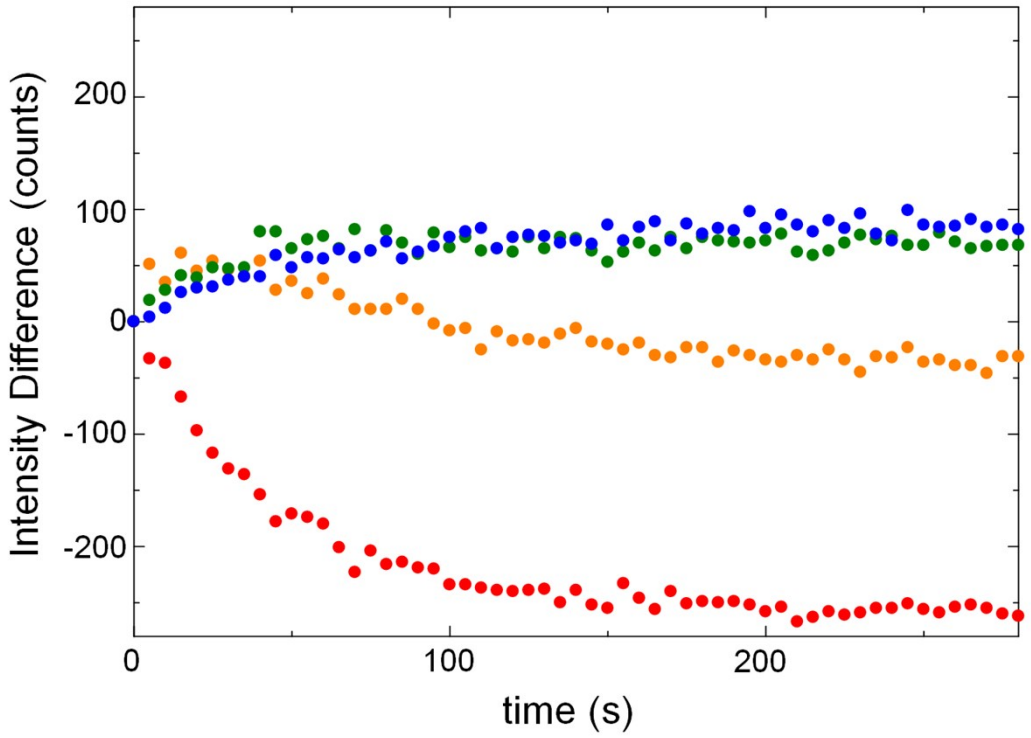

Figure S6. Chronological change in fluorescent intensity at various wavelengths: 600 nm (red), 550 nm (orange), 500 nm (green), and 450 nm (blue).

8. Chronological Change of 1□DMASP after the end of laser irradiation

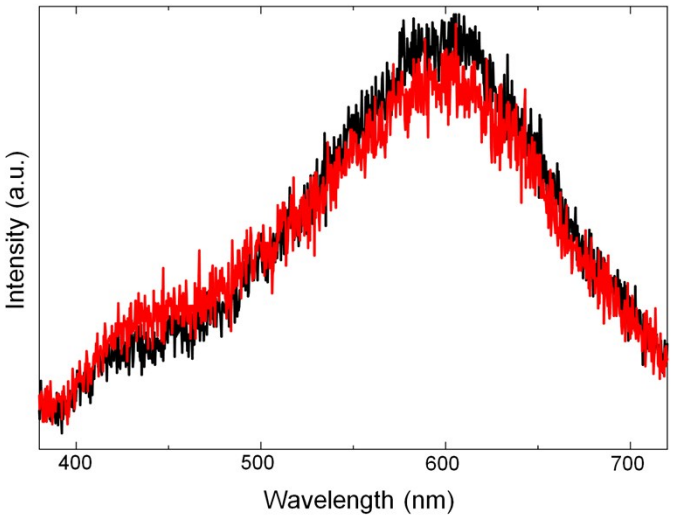

Figure S7. Fluorescent spectrum of 1□DMASP after pulsed laser exposed for 20s (black line). After the pulsed laser irradiation was stopped, the fluorescent spectrum of **1**□DMASP was collected again after 15 min (red line).

9. Irradiation of 1□DMASP and 1□DMASP$_{half}$ by CW laser

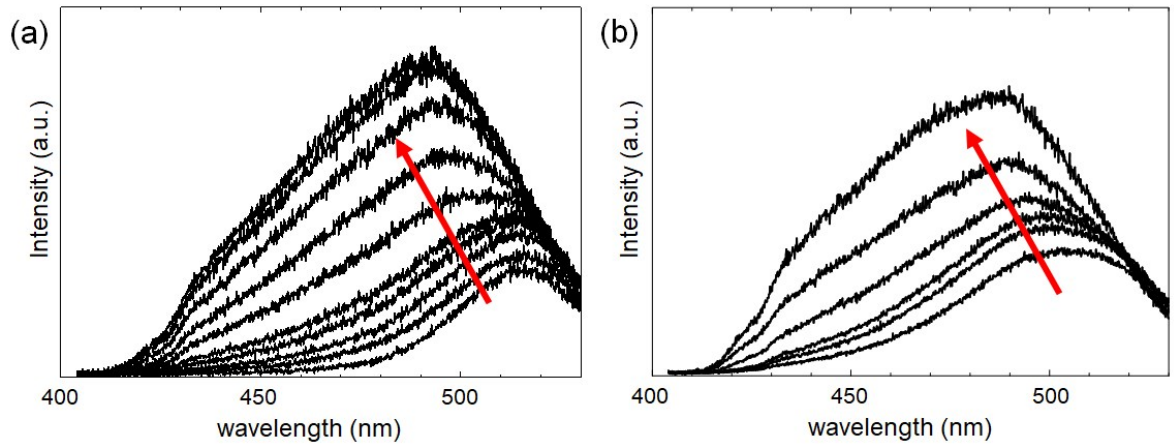

Figure S8. Fluorescent spectra of (a) **1**□DMASP after CW laser irradiation (375 nm) for various exposure times: 0, 5, 10, 20, 30, 60, 90, 120, 150, and 180 s, and (b) **1**□DMASP$_{half}$ after CW laser irradiation (375 nm) for various exposure times: 0, 10, 20, 30, 60 and 90.

10. Reversibility of emission colour change of 1□DMASP

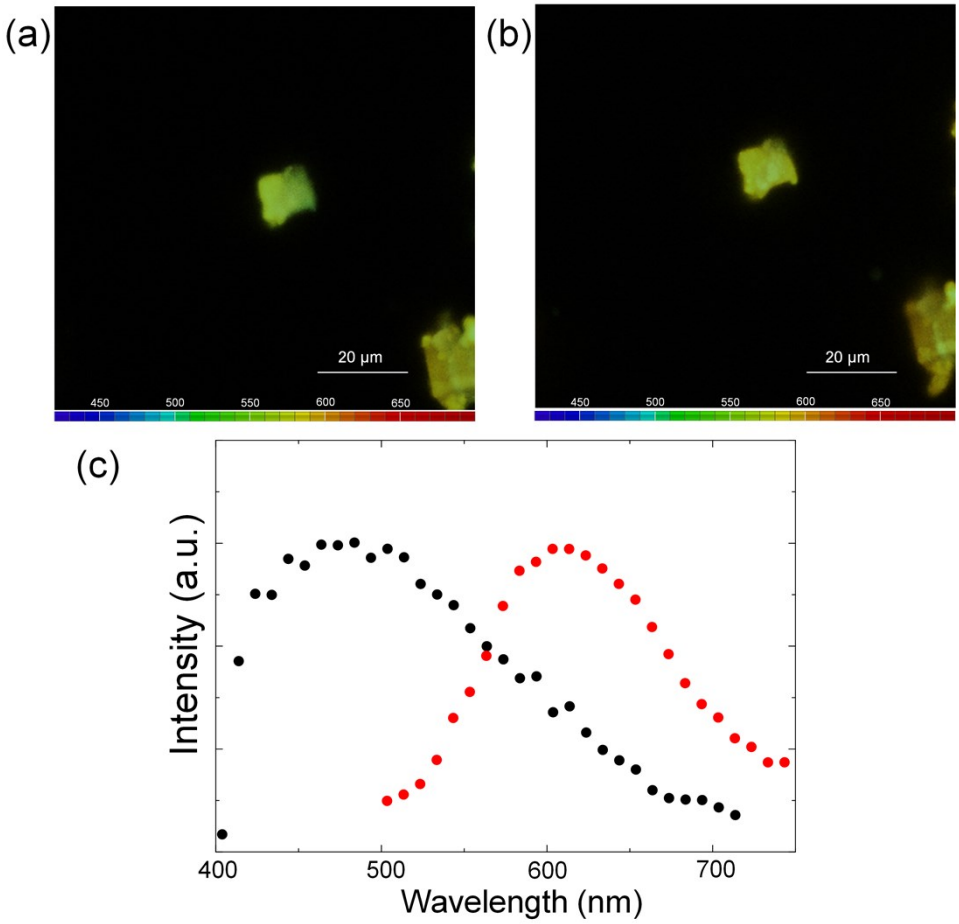

Figure S9. Laser scanning microscopy images of **1**□DMASP (a) after pulse laser irradiation, and (b) after subsequent heating at 150 °C for 2 h. (c) Fluorescent spectra of **1**□DMASP after pulse laser irradiation (black dots) and after subsequent heating (red dots).

11. References

S1 M. Elstner, D. Porezag, G. Jungnickel, J. Elsner, M. Haugk, T. Frauenheim, S. Suhai, and G. Seifert. *Phys. Rev. B*, 1998, **58**, 7260.

S2 Y. Yang, H. Yu, D. York, Q. Cui, and M. Elstner, *J. Phys. Chem. A* 2007, **111**, 10861–10873.

S3 B. Aradi, B. Hourahine, and Th. Frauenheim, *J. Phys. Chem. A*, 2007, **111**, 5678-5684.

S4 (a) M. Gaus, A. Goez, M. Elstner, *J. Chem. Theory Comput.* 2013, **9**, 338–354; (b) M. Kubillus, T. Kubař, M. Gaus, J. Řezáč, M Elstner, *J. Chem. Theory Comput.* 2015, **11**, 332–342.

S5 S. Grimme, J. Antony, S. Ehrlich, and H. Krieg, *J. Chem. Phys.* 2010, **132**, 154104.

S6 D. N. Dybtsev, H. Chun and K. Kim, *Angew. Chem. Int. Ed.*, 2004, **43**, 5033–5036.

S7 S. Dapprich, I. Komaromi, K. S. Byun, K. Morokuma, and M. J. Frisch, *J. Mol. Struct.: THEOCHEM* 1999, **461**, 1−21.

S8 T. Vreven, K. S. Byun, I. Komaromi, S. Dapprich, J. A. Montgomery, K. Morokuma, and M. J. Frisch, *J. Chem. Theory Comput.* 2006, **2**, 815−826.

S9 M. J. T. G. W. Frisch *et al.* Gaussian 09, Revision D.01; Gaussian, Inc.: Wallingford, CT, 2013.

S10 M. E. Casida in *Recent Developments and Applications in Density- Functional Theory*, (Eds: Seminario JM), Amsterdam, The Netherlands: Elsevier, **1996**, pp. 155-92.

S11 A. K. Rappe, C. J. Casewit, K. S. Colwell, W. A. Goddard, and W. M. Skiff, *J. Am. Chem. Soc.* 1992, **114**, 10024−10035.

S12 T. R. Lucas, B. A. Bauer, and S. Patel, *Biochim. Biophys. Acta, Biomembr.* 2012, **1818**, 318−329.

S13 M. Sowmiya, A. K. Tiwari, Sonu and S. K. Saha, *J. Photochem. Photobiol. A Chem.*, 2011, **218**, 76–86.